Expert Systems With Applications 232 (2023) 120879

Contents lists available at ScienceDirect

Expert Systems With Applications

journal homepage: www.elsevier.com/locate/eswa

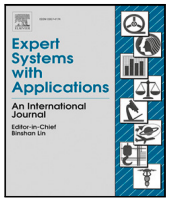

Emergent multipath COVID-19 specimen collection problem with green corridor through variable length GA

Somnath Maji [a,*], Kunal Pradhan [b], Samir Maity [c], Izabela Ewa Nielsen [c], Debasis Giri [d], Manoranjan Maiti [e]

[a] Department of Computer Science & Engineering, Maulana Abul Kalam Azad University of Technology, Nadia 741249, W.B., India
[b] Department of Computer Science & Engineering, Tezpur University, India
[c] Department of Materials and Production, Operations Research Group, Aalborg University, Aalborg, 9220, Denmark
[d] Department of Information Technology, Maulana Abul Kalam Azad University of Technology, Nadia 741249, W.B., India
[e] Department of Applied Mathematics with Oceanography and Computer Programming, Vidyasagar University, West Bengal, India

ARTICLE INFO

Keywords:
COVID-19
False negative
TSP
Green corridor
Variable length chromosome GA

ABSTRACT

The COVID-19 pandemic has spread worldwide exponentially. Typically, for testing, a provincial main government hospital cum testing center collects patients' specimens from remote health centers in the minimum possible time, satisfying the 'false negativity' constraint of the first collected specimen. With infrastructural developments throughout the world, multiple paths are available for transportation between two cities. Currently, the 'green corridor' is used for the transportation of human organs to be implanted, travel of VIPs, etc., in the minimum possible time. Taking these facts in consideration, for the first time, a green corridor system is suggested to provide a transportation pathway from small hospitals and urban/rural health centers to the testing center with COVID-19 specimens such as blood, nasal and throat swabs, and viral RNA, within the first collected specimen's life period. As health centers are located in different places, appropriate routing plans are needed for visiting them in the minimum possible time. A problem arises if this routing time exceeds the 'false negativity' of the first collected specimen. Thus, multipath COVID-19 specimen collection problems (MPC-19SCPs) are mathematically formulated to be collected from all health centers, and optimum routing plans are obtained using fixed and variable length genetic algorithms (VLGAs) developed for this purpose. For the first time, green corridor systems are suggested to incorporate the centers. The objectives of the models are, subject to the 'false-negative'' constraint, minimization of the system time (Model A) and the green corridor time without or with mutual cooperation among the minimum number of centers for the transfer of specimens (Models B and C, respectively). The developed algorithms are based on variable length chromosomes, probabilistic selection, comparison crossover and generation-dependent mutation. Some benchmark instances from TSPLIB are solved by VLGA and GA. The competitiveness of VLGA is established through ANOVA. The models are numerically demonstrated, and some conclusions are derived.

1. Introduction

COVID-19 is becoming more infectious in its third wave across the globe where the population density is very high (Kannan et al., 2021).

The government of India has made the decision to perform rapid tests as often as possible to identify affected persons, isolate such individuals from the rest of the population and then treat them for recovery (Halder et al., 2022). As the COVID-19 test kits are costly and not widely available, the government of the province of West Bengal has identified some major hospitals as testing-cum-treatment centers for COVID-19 (Fig. 1(a), for example). The clinical specimens of a COVID-19 patient are oropharyngeal, throat, and nasopharyngeal swabs, blood, etc. (Adigal et al., 2021). These specimens are collected from rural health centers and brought to major hospitals for testing. The major hospitals in rural areas are also not well equipped and have several resource constraints, such as only one AC-equipped medical van for the collection of specimens. Thus, the arrangement between the major hospital and its corresponding health centers is as follows: A well-equipped vehicle starts from the major hospital, visits the health centers under it, takes the collected specimens at the centers and then returns to the starting hospital in the minimum possible time

* Corresponding author.
E-mail addresses: somnathmajivucs@gmail.com (S. Maji), kunalpradhan86@gmail.com (K. Pradhan), maitysamir13@gmail.com (S. Maity), izabela@mp.aau.dk (I.E. Nielsen), debasis_giri@hotmail.com (D. Giri), mmaiti2005@yahoo.co.in (M. Maiti).

https://doi.org/10.1016/j.eswa.2023.120879
Received 23 October 2022; Received in revised form 5 April 2023; Accepted 17 June 2023
Available online 22 June 2023

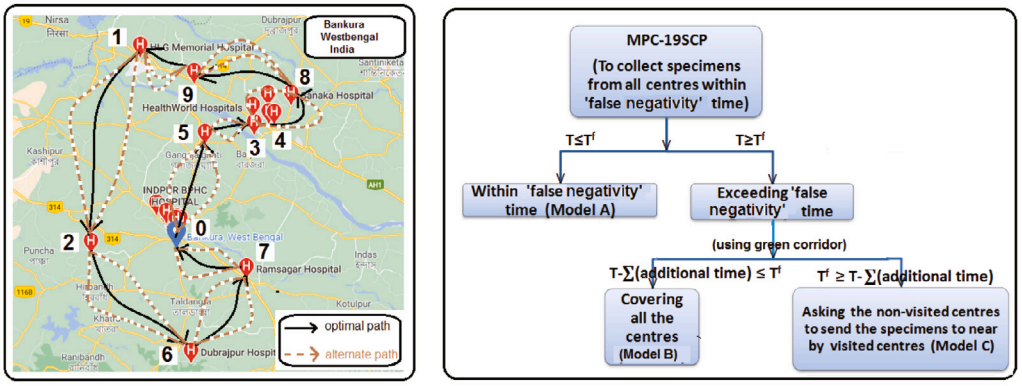

(a) Optimal path of MPC-19SCP for Bankura district (b) Schematic representation of the proposed models.

Fig. 1. Optimal path and schematic representation of the proposed models.

following an optimum routing plan and satisfying the time constraint ('false-negative'). This process is followed daily. This is a traveling salesman problem (TSP)-type $NP-hard$ problem (Saji & Barkatou, 2021). Here, the system also demands that specimens from all the health centers (nodes) be collected within the 'false negativity' constraint of collected specimens. This 'false negativity' time is counted with respect to the first collected specimen from the first visited health center. The main goal of this investigation is to visit all the health centers within 'false-negative' time with/without mutual cooperation among some centers, if required. First, attempt is made to visit and collect specimens from all centers within the 'false negativity' of the first collected specimen. If it is not possible due to 'false negativity', two alternatives are suggested to visit all the health centers satisfying the 'false negativity' constraints returning through a green corridor (i) without or (ii) with some centers mutual cooperation. Generally, the traveling time includes some additional time due to traffic signals, toll plazas, etc. However, these additional times are eliminated once a green corridor is created. Due to the development of infrastructure (roads, overpasses, bridges, etc.), alternate travel paths are available between different places. Thus, there are several route connections between the main hospital and the centers and among the centers. To address these issues, multipath COVID-19 specimen collection problems (MPC-19SCPs) without/with green corridors are formulated under different real-life scenarios and solved by developed variable and fixed length chromosome-based genetic algorithms (VLGA and GA). There have been several research papers on the different effects of COVID-19, such as on the economy (Kumar et al., 2022), manufacturing (Gamal et al., 2022), tourism (Zhang & Tian, 2022), and unemployment (Perboli & Arabnezhad, 2021), but none has considered the above important COVID-19 specimen collection problem in the rural areas of developing countries.

A green corridor system is typically one way to expedite organ transplants and save lives. In this system, the traffic department collaborates to transport a vital organ in less than 60 – 70% of the time usually taken to go from place A to place B. This system was first devised to handle medical emergencies. A green corridor is a special route that is managed in such a way that all traffic signals on the route connecting two specific (organ donating and harvesting) hospitals are green and controlled manually. In India, the concept of green corridors has been used since 2014.

Currently, throughout the world, significant infrastructural development is taking place in terms of roads, etc., for transportation. There are several roads connecting two cities/places. For instance, during 2000–12, India, a developing country, launched 'Golden quadrilateral highways projects' (Asturias et al., 2019) to connect its large/important cities. Also in 2000, India launched 'Pradhan Mantri Gram Sadak Yojana' (Wagale et al., 2020) to develop the connecting roads between main cities and semiurban/rural business centers/medical hubs as part of a poverty reduction strategy. Similarly, there has been development in road freight transportation systems worldwide. Thus, for travel/routing, a medical vehicle/ambulance will have more than one possible road to take from one medical center to another.

All these facts prompted us to make the following queries in connection with MPC-19SCPs. As the COVID-19 specimens are collected from rural health centers, how can they then be brought to the main hospital maintaining their 'false-negative' time period? What is the optimal route plan if the 'false-negative' constraint is violated? In this case, how can specimens be collected from all health centers with only one vehicle? Can the concept of a green corridor be utilized for return to cover all health centers? Even if this is not possible using the green corridor, what additional arrangements can be made taking the major hospital's resource constraints (only one collecting vehicle) into consideration? At the tactical level, how can the green corridor be implemented with minimum public inconvenience? How can the entire travel plan be made using a single convenience so that the total time and/or cost are minimized within the given 'false-negative' constraint? All these operations should be completed within the lifespan of the collected specimens. Considering the above questions, an attempt has been made to formulate and solve the emergent problems in collection of COVID-19 specimens in different situations.

In this paper, for the collection of COVID-19 specimens from remote rural health centers and their transport to the testing hospital with one collecting vehicle (due to resource constraints), we present three models based on the specimens' 'false negativity' constraint. Here, the lifetime of the first collected specimen is taken as the 'false-negative' time. In developing countries such as India, testing of COVID specimens is normally performed centrally at a slightly better-equipped hospital, with specimens brought from different rural health centers that operate independently during the same working hours. Taking this into consideration, routing plans for specimen collection are suggested. There may be two cases: (i) Within the 'false-negative' time, after covering all the health centers, the vehicle is able to return to the testing center (Model A). (ii) The above proposition is not feasible. In this case, if the vehicle has to return to the main hospital to satisfy the 'false negativity' constraint, the vehicle will skip some health centers, which is not at all desirable. In this case, to obtain the specimens from all the centers, we propose two alternatives: (iia) In addition to the road coverage time, some additional time is accounted for in routing due to congestion, traffic control, toll tax collection, etc. Without this additional stoppage time, the system of nonstop transportation is called a 'green corridor' (GC). The general population is somewhat inconvenienced by the imposition of a green corridor transportation system. Hence, to minimize

public inconvenience, we minimize the green corridor time to cover all health centers within the 'false-negative' time, if possible (Model B). (iib) After the introduction of the green corridor, if it is not possible to cover all health centers within the 'false-negative' time, then we maximize the number of visited centers using the green corridor, and the remaining (minimum) centers are asked to send their specimens to their nearest centers included in the green corridor plan (Model C).

Here, a variable-length GA (VLGA) with probabilistic selection, comparison crossover and generation-dependent mutation is developed to solve the proposed MPC-19SCP models along with some benchmark instances from TSPLIB (Reinelt, 1991). The supremacy of VLGA is also statistically established.

Novelties in this investigation are as follows:

- Multipath COVID-19 specimen collection problem with/without a green corridor (GC)
- These are formulated with the false-negative constraint based on the first collected specimen
- For minimum public inconvenience, GC time is minimized, covering all health centers.
- Models are solved by a variable-length chromosome-based genetic algorithm (VLGA).
- VLGA incorporates probabilistic selection, comparison crossover, and generation-based mutation.

The paper is organized as follows: Sections 1 and 2 provide a concise introduction with motivation and a brief literature review, respectively, Section 3 gives mathematical formulations of MPC-19SCP models. The proposed algorithm is explained in Section 4. The validity of the proposed algorithm is addressed in Section 5. Some real-life experiments and a brief discussion are presented in Section 6. Finally, Section 7 concludes the paper and discusses the scope of potential future research.

2. Background and literature review

Organ transportation is a crucial challenge in developing countries (Nguyen et al., 2020). Similarly, in the present pandemic period, the collection of specimens from remote health centers and transportation to the main hospital for testing within the 'false-negative' constraint of the first collected specimen is a difficult task. Bellotti and Francoso (2021) investigated how efficiently human organ transportation is performed in different countries under ischemia time (in which organs can survive without blood perfusion). They considered fixed/known starting and ending points, where the path between those points is assisted by flight in emergent requirements. This is a form of 'green corridor' that is considered in the present investigation. Bruni et al. (2006) focused on location–allocation problems, mainly in a case study of Italy. The authors investigated only the reduction of 'wasted organs' with the help of a mathematical model considering different real-life constraints. Another case study was presented by Zahiri et al. (2014) for Iranian organ transplants where possibilistic programming models were designed. They derived a multiperiod location–allocation problem of organ transplantation under an uncertain supply chain. The researchers minimized the system cost with the help of time constraints. Ambulance, VIP, police patrol, and fire service vehicles all work together in an emergency situation. In reaching their destinations in time, they face different problems (traffic congestion, rail crossings, etc.) in routing. To overcome these situations, Dhatrak and Gandhe (2018) investigated and solved using IoT for clearing traffic when this vehicle reaches the signal. This is a type of green corridor that we employ in the current article. In emergency/war/disaster situations (Walia et al., 2018), using unmanned aircraft vehicles, the system cost is minimized considering the distance, equipment cost, environmental conditions, and other risk factors. To our knowledge, no other study has considered the problem of COVID-19 specimen collection routing from different remote health centers to the main hospital for testing. Additionally, none has maximized the number of visited centers while satisfying the 'false-negative' constraint. Some emergent routing investigations are listed in Table 1.

Table 1
Applications of emergent routing.

Applications of emergent routing	Methods
Human organs transportation (Nguyen et al., 2020, Bellotti & Francoso, 2021)	Review, EOS
Location–allocation problems (Bruni et al., 2006)	Lingo
Multi-period location–allocation (Zahiri et al., 2014)	Possibilistic
VIP Vehicle, Fire service (Dhatrak & Gandhe, 2018)	IoT
Emergent/war/disaster situation (Walia et al., 2018)	Simulation
Emergency medical services (Aringhieri et al., 2017)	Review paper
Post-disaster transportation (Wang et al., 2016)	Hybrid ACO, GA
TSP with drone station (Kim & Moon, 2018)	Decomposition
Capacitated VRP (Wang et al., 2019, Abu-Monshar et al., 2022)	Local search, Agent-based
Ambulance medical service (Ziya-Gorabi et al., 2022)	Fuzzy chance-constrained
Relief distribution (Zhang, Li et al., 2022)	Approximation
Medical emergency (Karpova et al., 2023)	Heuristic algorithms

For routing problems–TSP (Wang & Wang, 2023; Zhang et al., 2023), VRP (Kuo et al., 2023; Rahmanifar et al., 2023), etc.- the heuristic method GA is frequently used (Di Placido et al., 2022; Zhang, Wang et al., 2022). In these problems, the chromosomes in GA are of fixed length. However, for solving TSP-type problems such as TPP, chromosomes are of variable lengths. In the models for collecting specimens within the 'false-negative' constraint, the chromosomes in GA may be of variable length. Few investigations have used variable-length chromosomes in evolutionary computations. Pawar and Bichkar (2015) introduced variable-length chromosome-based GA and generated classification rules to solve network intrusion detection problems. They used variable-length chromosomes with roulette wheel selection, one-point crossover and random mutation. A VLGA (Qiongbing & Lixin, 2016) was developed with the same adjacency crossover operation and applied to path optimization. Anwit and Jana (2018) developed a GA with different chromosome lengths, one-point crossover, and chromosome length-dependent mutation to optimize the data collection for the sensor network. They studied the optimal number of locations of the mobile sink using the variable number of chromosomes (population size) in GA. Traffic coordination at a multipath traffic point for heterogeneous vehicles was studied with vehicle arrival sequencing through VLGA (Cruz-Piris et al., 2019). The researchers introduced a new crossover operation strategy based on the parents' length.

Maity et al. (2015) proposed comparison crossover in GA for TSP. They used comparison (minimum value) between two edges to produce offspring. We extend this comparison procedure among three successive edges in this investigation. Although complexity increases, overall performance is improved. Here, we use VLGA with probabilistic selection, three-edged comparison crossover and generation-dependent mutation, which has not been used by the investigations thus far.

3. Proposed multipath COVID-19 specimen collection problem (MPC-19SCP)

3.1. Nomenclature

Some basic notations are presented in Table 2.

3.2. Multipath TSP (3DTSP)

In the formulation of the usual TSP (2DTSP), there is only one route for travel from the ith to the $(i+1)th$ centers. Currently, there are a number of routes (more than one, 3DTSP) for this purpose. Let

Table 2
Notations with descriptions.

Notation	Description
N	Total number of nodes/city/center, ($N = 1$ is depot)
i, j	Index set (i, j = 1, 2, 3, …, N)
K	Maximum visited center ($K \leq N$)
Q	Set of nodes {1, 2, 3, …, N}
R	Set of routes $r \in$ {1, 2, 3, …,R}
x_i	ith visiting center
$dis(x_{(i)(i+1)}, r)$	Distance between ith to $(i+1)$th center using $r \in R$ route
$c(x_{(i)(i+1)}, r)$	Travel cost from ith to $(i+1)$th center using $r \in R$ route per unit distance
$t(x_{(i)(i+1)}, r)$	Time taken for travel (actual vehicle running time) from ith center to $(i+1)$th center using $r \in R$ route
$t^A(x_{(i)(i+1)}, r)$	Additional time taken for travel from ith center to $(i+1)$th center using $r \in R$ route
w_i	Available specimens at ith center
W	Total amount of collected specimens
T	Total time for the system
T^K	Total time upto the Kth node
T^f	'false negative' time/life span of the specimens
T^G	Green corridor time
τ_i	Loading time of specimens at ith center
G'	Number of green corridor segment
$f(X_i)$	Fitness of the ith chromosome
P_B^i	Probability of ith chromosome
Ch_i	ith chromosome
x_{ijr}	Binary decision variable, $x_{ijr} = 1$ for the travel from ith to jth center using r route, else, $x_{ijr} = 0$
γ_{ijr}	Binary decision variable, $\gamma_{ijr} = 1$ for active green corridor else, $\gamma_{ijr} = 0$

$c(x_i, x_{i+1}, r)$ be the travel cost from the ith to $(i+1)th$ centers using rth route. Thus, the multipath TSP is mathematically represented as:

$$\text{Min} \quad Z = \sum_{i=1}^{N}\sum_{j=1}^{N}\sum_{r=1}^{R} c_{ijr}x_{ijr} \tag{1}$$

$$where\ x_i \neq x_j, i, j = 1, 2, \ldots, N,\ r \in \{1, 2, \ldots, R\}.$$

$$\text{subject to} \quad \sum_{i=1}^{N}\sum_{r=1}^{R} x_{ijr} = 1 \ \text{ for } j = 1, 2, \ldots, N \qquad \sum_{j=1}^{N}\sum_{r=1}^{R} x_{ijr} = 1 \ \text{ for } i = 1, 2, \ldots, N \tag{2}$$

with

$$\sum_{i\in S}\sum_{j\in S} x_{ijr} \leq |S| - 1, \forall S \subset Q \tag{3}$$

$$where\ \ x_{ijr} \in \{0, 1\}, i, j = 1, 2, \ldots, N.\ r \in \{1, 2, \ldots, R\}.$$

The objective function (1) can be rewritten as:

Determine a complete tour $(x_1, x_2, \ldots, x_N, x_1)$,

$$\text{Min} \quad Z = \sum_{i=1}^{N-1} c(x_{(i)(i+1)}, r) + c(x_{(N)(1)}, r) \tag{4}$$

$$where\ x_i \neq x_j, i, j = 1, 2, \ldots, N,\ r \in \{1, 2, \ldots, R\}.$$

Here, Eq. (4) stands for the minimization of the travel cost/time/distance. The first two constraints in Eq. (2) imply the visiting of a node only once, and Eq. (3) eliminates the subroute.

3.3. Multipath COVID-19 specimen collection problems (MPC-19SCPs)

3.3.1. Formulation of models

There are three possibilities (Fig. 1(b)) in the case of routing. (i) The total routing time is less than the 'false-negative' time. In this case, after collecting specimens from all health centers, the medical van returns to the main hospital within the said 'false-negative' time (Model A). (ii) The total routing time is more than the 'false-negative' time. (iia) To reduce the routing time, a GC (without additional times due to signals, etc.) is imposed on the optimum routing path. In this case, the routing time with the GC is less than the 'false-negative' time, and to reduce public inconvenience, the GC time is minimized (Model B). (iib) After a total GC imposition, if routing time > 'false-negative' time, unvisited centers are identified and asked to send their specimens to near-by centers lying on the routing path. In this case, the number of visited centers is maximized (Model C).

3.3.2. Model A: MPC-19SCP for minimum total time

Let specimen collection and delivery to the testing facility center be performed within the 'false-negative' time, which is considered a constraint. In this model, the vehicle's route is determined for the minimum total system time.

The health worker makes a complete tour $(x_1, x_2, \ldots, x_N, x_1)$ with $r(\in R)$ routes for

$$\text{Min } T = \sum_{i=1}^{N-1} [t(x_{(i)(i+1)}, r) + t^A(x_{(i)(i+1)}, r) + \tau_{(i+1)}] + t(x_{(N)(1)}, r) + t^A(x_{(N)(1)}, r) \tag{5}$$

subject to

$$T - [t(x_{(1)(2)}, r) + t^A(x_{(1)(2)}, r)] \leq T^f \tag{6}$$

$$where\ \ \tau_1 = 0; i, j = 1, 2 \ldots N; r \in \{1, 2 \ldots, R\}. \tag{7}$$

The objective function in Eq. (5) has three parts: The first part is for the travel time (t), i.e., actual vehicle running time; the second part is for additional time (t^A) (traffic, toll plazas, etc.); and the third part is the vehicle stay time/loading time (τ) of the specimens at the center. The collected specimens must be delivered to the testing center within the 'false-negative' time T^f (WHO, 2020). Therefore, the constraint in Eq. (6) is applied with respect to the first collected specimen.

Management may also want to know the corresponding cost incurred in this process. The travel cost is given by

$$Z = \sum_{i=1}^{N-1} c(x_{(i)(i+1)}, r) * dis(x_{(i)(i+1)}, r) + c(x_{(N)(1)}, r) * dis(x_{(N)(1)}, r) \tag{8}$$

3.3.3. Model B: Covering all the centers with a green corridor

In this case, the 'false-negative' constraint is violated if specimens are collected from all the centers. To satisfy the constraint, the green corridor approach is introduced. The total routing time includes the congestion time, time due to traffic control, etc., at different places, the sum total of which is substantial. Let these times be called 'additional time'. If additional time is saved through the green corridor system, specimens may be collected from more health centers. In Model B, we determine the minimum green corridor time (T_G) of the system (here, the green corridor is imposed toward the end of the tour sequentially), so that specimens are collected from all the health centers within the 'false-negative' time and public inconvenience is minimum.

The MPC-19SCP model with corresponding green corridor minimization (Eq. (9)) is:

$$\text{Min } T_G = T - [t(x_{(1)(2)}, r) + t^A(x_{(1)(2)}, r)] - T^f \tag{9}$$

subject to

$$T - [t(x_{(1)(2)}, r) + t^A(x_{(1)(2)}, r)] > T^f, \tag{10}$$

$$T - [t(x_{(1)(2)}, r) + t^A(x_{(1)(2)}, r)] - (\gamma_{(N)(1)}, r) * t^A(x_{(N)(1)}, r) - \sum_{j=1}^{G} (\gamma_{(N-j)(N-j+1)}, r) * (t^A(x_{(N-j)(N-j+1)}, r)) \leq T^f, \quad (11)$$

$$where \quad G = min\{1, 2, \ldots, N-2\}, G' = 1 + G \quad (12)$$

along with the condition (7).

The objective function in Eq. (9) evaluates the minimum green corridor time for the entire tour. If the routing time exceeds the 'false-negative' time, considered from the first specimen collection node (Eq. (10)), then that extra time (routing time from first specimen collection center - 'false-negative' time) is adjusted using the green corridor by reducing the additional time (Eq. (11)). The total time interval of the imposed green corridor is evaluated through Eq. (12). Here, $G' = G + 1$ represents the green corridor segment up to the last center and from the last center to the testing hospital.

Management may also want to calculate the corresponding cost incurred in this process. This is given in Eq. (8).

3.3.4. Model C: Asking some centers unvisited to send the specimens to nearby centers lying on the green corridor

In this case, the 'false-negative' time is also greater than the system time, and it is so even after additional time becomes available due to the imposition of a GC. To overcome this situation, after the GC is created, we maximize the number of visited health centers within the 'false negativity' constraint, and the left-out centers are asked to send their specimens to nearby visited centers.

The health worker makes a tour (x_1, x_2, …, x_K, x_1) with r routes. Here, visited centers (K) are less than or equal to the total number of centers ($K \leq N$) along the green corridor, and the remaining centers (N-K) are asked to send their specimens to nearby centers.

To find a nearby center: Let S = $\{s_1, s_2, \ldots, s_{N-K}\}$ be the set of unvisited centers and their nearby centers be L = $\{k_1, k_2, k_3, \ldots, k_K\}$. Nearby centers are found under the following condition.

$$t(x_{(s)(k)}, r) + t^A(x_{(s)(k)}, r) \leq \sum_{i=1}^{k} [t(x_{(i)(i+1)}, r) + t^A(x_{(i)(i+1)}, r) + \tau_{(i+1)}] \quad (13)$$

$$where, \quad dis_{sk} = min\{dis(x_{(s)(k)}, r)\}, \quad s \in (N-L), \quad k \in L$$

The mathematical formulation of Model C is as follows.

$$\text{Max } K \quad (14)$$

$$\text{where } T_G = T^K - [t(x_{(1)(2)}, r) + t^A(x_{(1)(2)}, r)] - T^f \quad (15)$$

subject to

$$T - [t(x_{(1)(2)}, r) + t^A(x_{(1)(2)}, r)] > T^f, \quad (16)$$

$$T^K - [t(x_{(1)(2)}, r) + t^A(x_{(1)(2)}, r)] > T^f, \quad (17)$$

$$T^K - [t(x_{(1)(2)}, r) + t^A(x_{(1)(2)}, r)] - (\gamma_{(K)(1)}, r) * t^A(x_{(K)(1)}, r) - \sum_{j=1}^{G} (\gamma_{(K-j)(K-j+1)}, r) * (t^A(x_{(K-j)(K-j+1)}, r)) \leq T^f, \quad (18)$$

$$T^K = \sum_{i=1}^{K-1} [t(x_{(i)(i+1)}, r) + t^A(x_{(i)(i+1)}, r) + \tau_{(i+1)}] + t(x_{(K)(1)}, r) + t^A(x_{(K)(1)}, r), \quad (19)$$

$$G = min\{1, 2, \ldots, K-2\}, \quad G' = 1 + G, \quad (20)$$

along with Eqs. (7) and (13).

The constraint Eq. (16) is applied with respect to the first collected specimens.

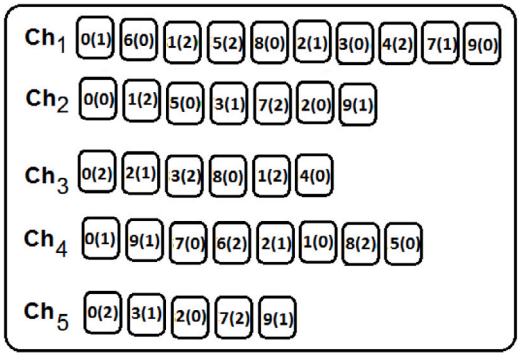

Fig. 2. Representation of five variable length chromosomes.

The objective function in Eq. (15) evaluates the minimum green corridor time for the entire tour. If the routing time exceeds the 'false-negative' time, considered from the first specimen collection node (in Eqs. (16) and (17)), then that extra time (routing time from the first specimen collection center minus 'false-negative' time) is adjusted using a green corridor by reducing the additional time (Eq. (18)), but if it is not possible to cover all the centers, then the remaining (minimum) centers are asked to send their specimens to nearby centers. The total number of green corridor segments is evaluated through Eq. (20).

Management may also want to determine the corresponding cost up to the Kth center + the cost incurred by the (N-K) number of centers to send their specimens to nearby centers in this process. This is given by Eq. (21).

$$Z = \sum_{i=1}^{K-1} c(x_{(i)(i+1)}, r) * dis(x_{(i)(i+1)}, r) + c(x_K, x_1, r) * dis(x_{(K)(1)}, r) + \sum_{s=1}^{N-K} c(x_{(s)(k)}, r) * dis(x_{(s)(k)}, r) \quad (21)$$

where, k represents the nearby centers of s, k ∈ {set of visited nodes}, s ∈ {set of non-visited (N-K) centers}.

4. Proposed variable-length genetic algorithm (VLGA)

To solve the proposed models, we develop a variable-length GA (VLGA). Although the proposed MPC-19SCP is TSP type, the consideration of the 'false-negative' constraint of the collected specimens forces the termination of the route (collection) without all the centers being visited (Model C). Therefore, the length of the chromosomes in GA varies with the routing plan (shown in Fig. 2). The proposed VLGA is developed with probabilistic selection, comparison crossover and generation-dependent mutation. Details of VLGA are as follows.

4.1. Representation

Here, M (pop size) routing paths among N nodes (centers) with different lengths are generated randomly satisfying the 'false negativity' constraint. Let the ith chromosome, defined as $X_i = (x_{i1}, x_{i2}, \ldots, x_{iK})$, be created with $x_{i1}, x_{i2}, \ldots, x_{iK}$, the K non-repeated nodes and $r \in R$ alternate paths in a tour. Here, x_{ij}, i = 1, 2, …, M and j = 1, 2, …, K(≤ N). The fitness of chromosomes is evaluated by summing the times/costs between the consecutive centers of each solution. The ith solution's fitness in the solution space is presented by $f(X_i)$. An example of variable-length chromosomes is given in Fig. 2.

Here, Ch_1, i.e., in the first chromosome (routing path), is 0(1)-6(0)-1(2)-5(2)-8(0)-2(1)-3(0)-4(2)-7(1)-9(0). This means that the collection vehicle starts from 0 (depot), moves to the 6th center using the 2nd path, and then moves to the 1st center using 1st path, after which it moves to the 5th center through the 3rd path and so on. Here, alternate paths between two centers are represented by 0 ($1st$), 1 ($2nd$) and 2 ($3rd$).

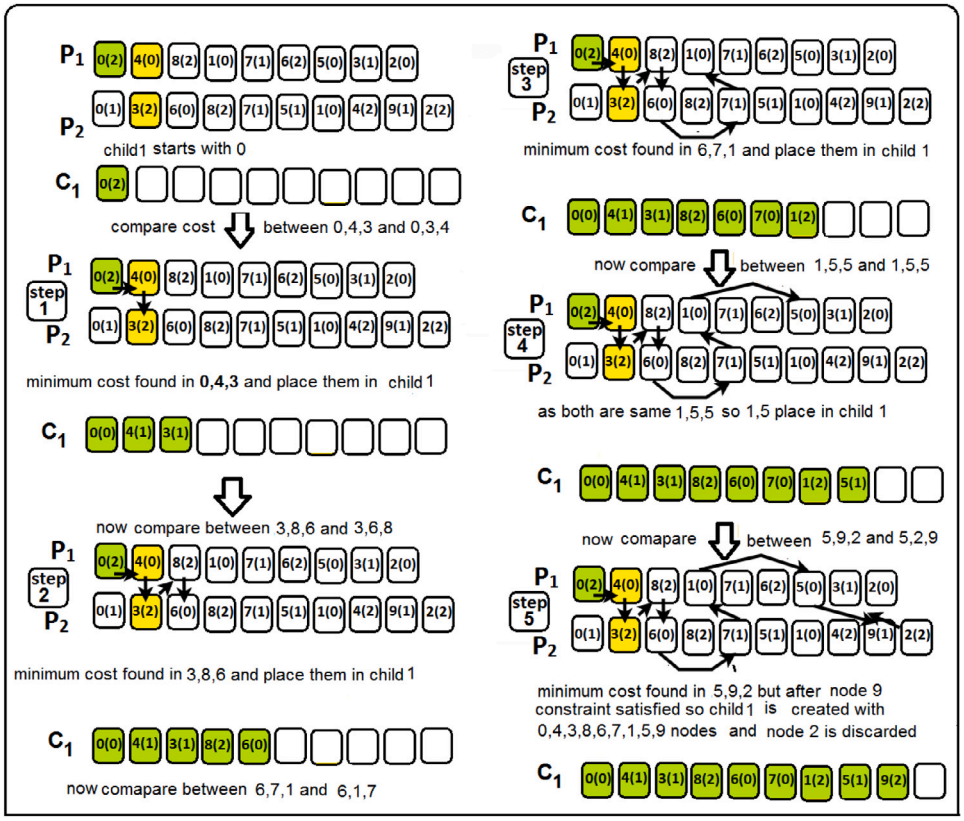

Fig. 3. Comparison crossover.

4.2. Probabilistic selection

In this section, a probabilistic selection (Maity et al., 2015) strategy is considered for generating the mating pool. The probability of the ith chromosome (P_B^i) is evaluated as

$P_B^i = e^{((f_{min}-f(X_i))/T)}$, $T = T_0(1-a)^k$, $k = (1 + 200 * (g/G))$, where f_{min} = chromosome with minimum fitness, g = current generation number, G = maximum generation number, T_0 = rand[25,250], a = rand[0,1]. To form the matting pool, a random number $r \in [0, 1]$ is generated against each chromosome, and if $r<P_B^i$, then the corresponding chromosome is selected.

4.3. Comparison crossover

First, check r ($\in rand[0, 1]$) < p_c (predefined), for each chromosome for matting pool. If it is true for a chromosome, then that chromosome is selected for the parent. Like this, select p_c*M parents, from which children will be generated. The comparison crossover approach for children generation is based on comparing the fitness of the chromosome taking two nodes together, one from each parent. Thus, a comparison is performed with a sequence of 3 nodes, as is illustrated below.

Let two parents, P_1 (chromosome length 9) and P_2 (chromosome length 10), be selected (cf. Fig. 3) with 0 (main hospital) as the starting and ending position. In step 1, compare sequences 0,4,3 and 0,3,4 with all alternate paths. Minimum fitness is found in 0,4,3 using 1st path from 0 to 4 and 2nd path from 4 to 3 (say). Therefore, place them into C_1 (child 1), and this becomes 0(0)-4(1)-3. Thus, alternate paths among them are also updated.

In step 2, compare the fitness between the sequences 3,8,6 and 3,6,8 with the alternate paths. If we say the minimum is 3,8,6 using 2nd path from 3 to 8 and 3rd path from 8 to 6, then place them into C_1 with updated multipath, and this becomes 0(0)-4(1)-3(1)-8(2)-6. Repeat the same process (steps 3, 4, and 5) until the termination criteria are satisfied. Finally, C_1 becomes 0(0)-4(1)-3(1)-8(2)-6(0)-7(0)-1(2)-5(1)-9(2)-0 (say) with 9 nodes.

For the second child (C_2), we rearrange the second parent (P_2) in reverse order (for both nodes and paths), as shown in Fig. 4. As the costs/times between the nodes are symmetric, this arrangement does not affect the chromosome's fitness value. The remaining procedures are the same as those for the first child.

The steps of the proposed comparison crossover are presented in Algorithm 1.

4.4. Generation-dependent (GD) mutation

4.4.1. Selection of the chromosomes for mutation

The probability of mutation p_m is generated based on different iterations. Here, p_m (by expression (22)) is dynamically updated at every generation (t). If r ($\in rand[0, 1]$) < p_m, then the corresponding chromosome is selected for mutation. The value of p_m decreases as generation progresses. This selection repeated for ($p_m * M$) times.

$$p_m = \frac{k}{t}, \qquad k \in rand(0, 1]. \tag{22}$$

4.4.2. Mutation process

Consider the selected ith chromosome $X_i = (x_{i1}, x_{i2}, \ldots, x_{iN})$. Now, generate two random numbers within [2, chromosome length]. For example, in Fig. 5, the selected chromosome for mutation is 0(2)-3(1)-5(0)-1(2)-7(2)-6(0)-4(1)-8(2)-2(0)-9(1)-0 (say). Consider two distinct random numbers, say 3 and 8, that are generated, i.e., the 3rd and 8th positions of the chromosome. Swapping between the 3rd and 8th positions also updates alternate paths, and the mutated chromosome becomes 0(2)-3(0)-8(1)-1(2)-7(2)-6(0)-4(2)-5(1)-2(0)-0. Due to 'false negativity', the length of the mutated chromosome may vary.

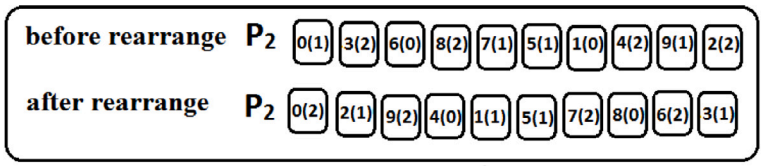

Fig. 4. Modified parent for second child.

Algorithm 1: Comparison crossover using variable length chromosomes

Input: Two parents P_1 and P_2 (P_1^i or P_2^j indicates i^{th} and j^{th} positions of the parents respectively)
Output: Two child's C_1 and C_2 (C_1^k or C_2^k indicates k^{th} position of the child)

Select distinct two parents (P_1, P_2) from mating pool
Initially P_1^0=P_2^0=C_1^0=0 (say) and i=1, j=1, k=1
for $k \leftarrow 1$ ***to*** N **do**
  while *(time (starts from first specimen collection)* $\leq T^f$*)* **do**
    if $((P_1^i \in C_1)$ **then**
      i=i+1
    if $((P_2^i \in C_1)$ **then**
      j=j+1
    if $(P_1^i == P_2^j)$ **then**
      Concatenate P_1^i in child 1 (C_1^k), k=k+1, and goto step 4
    if $(cost(P_1^{i-1}P_1^iP_2^j)) \leq cost(P_1^{i-1}P_2^jP_1^i))$ **then**
      Concatenate $P_1^iP_2^j$ in child 1 (C_1^k) and k=k+2
    else
      Concatenate $P_2^jP_1^i$ in child 1 (C_1^k) and k=k+2
Variable length child (C_1) created // similar for C_2

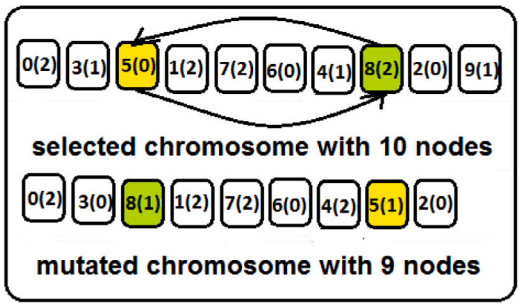

Fig. 5. Graphical representation of generation dependent mutation.

4.5. Algorithm for the proposed VLGA

The proposed VLGA is presented in Algorithm 2 and flowchart given in Fig. 6.

4.6. Complexity analysis

4.6.1. Time and space complexities

The time complexity of GA for TSP depends on the pop-size (M) and numbers of nodes (N). It is O(MN). Here, for the proposed VLGA, it is O(MN^2). The space complexity of VLGA is O(MN).

Algorithm 2: Variable length genetic algorithm (VLGA)

Input: Max-gen, population size, p_c, p_m, problem data, Total centers (N), Path-length=K (cover centers), Total uncover center (s)=N-K, Min=Large value
Output: optimal/near optimal solutions

Initialization as subsection 4.1
Set starting generation $t \leftarrow 1$
while *(*$t \leq$ *Max-gen)* **do**
  Probabilistic selection according to subsection 4.2
  Generate the mating pool
  Select distinct two parents from mating pool
  Comparison crossover according to subsection 4.3
  Generate and stored offsprings
  p_m evaluated from subsection 4.4.1
  GD mutation according to subsection 4.4
  Update the fitness and stored
if *(*$T < T^f$*)* **then**
  (Model A) Store the global optimum and near optimum values
  else
    if *(Eq. (11) satisfied)* **then**
      // (Perform through Model B) (green corridor)
      T_G=T-$[t(x_{(1)(2)}, r) + t^A(x_{(1)(2)}, r)] - T^f$
      j=0
      $T_G = T_G$-$(t^A(x_{(N-j)(N-j+1)}, r))$
      T_G^{count}=1
      while *(*$T_G \geq 0$*)* **do**
        T_G^{count}=T_G^{count}+1
        j=j+1
        T_G=T_G-$(t^A(x_{(N-j)(N-j+1)}, r))$
      Total Green corridor interval= T_G^{count}
      else
        // (Perform through Model C)
        for $c \leftarrow 1$ ***to*** s **do**
          for $j \leftarrow 1$ ***to*** K **do**
            E_{cost}=cost(s,j)
            if *(*$E_{cost} \leq$ *Min)* **then**
              Min=E_{cost}
              Selected node (j)
          Connected s with selected node j
          Total cost=Total cost+Min

5. Validity of the proposed algorithm

5.1. Test results for benchmark instances using VLGA GA-I

The performance of the proposed VLGA is established by solving 15 standard benchmark problems from TSPLIB (Reinelt, 1991). For

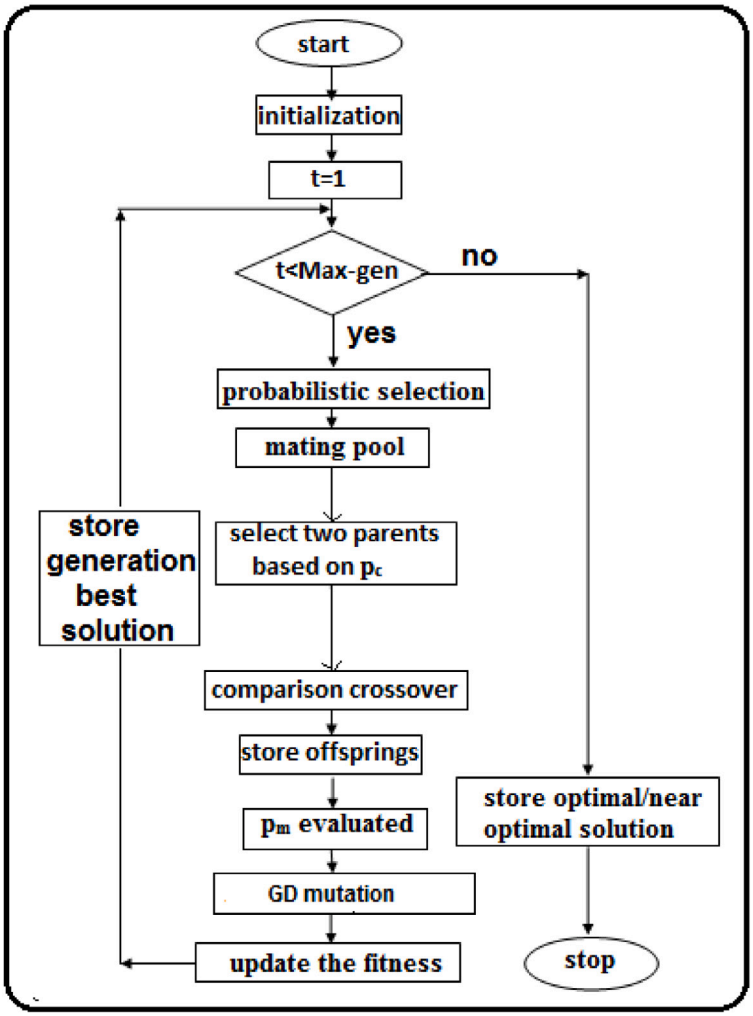

Fig. 6. Flowchart of VLGA.

Table 3
Results of TSPLIB instances using VLGA and GA-I.

Instances	BKS[a]	VLGA			GA-I		
		BFS[b]	Iteration	Time	BFS	Iteration	Time
gr17	2085	2085	79	0.07	2085	91	0.15
gr21	2707	2707	172	0.10	2707	184	0.22
gr24	1272	1272	184	0.12	1272	210	0.28
bays29	2020	2020	198	0.18	2020	168	0.59
hk48	11 461	11 461	279	0.48	11 461	312	0.97
eil51	426	426	312	0.67	426	362	2.25
brazil58	25 395	25 395	512	0.97	25 395	511	3.14
st70	675	675	572	1.72	675	593	4.26
eil76	538	538	618	1.96	538	680	4.31
eil101	629	629	890	3.74	629	1245	4.21
gr120	6942	6942	916	4.53	6942	1429	6.87
kroB200	29 437	29 437	1413	6.65	30 125	1814	9.37
a280	2579	2579	1610	8.29	2851	1968	11.61
pr1002	259 045	299 479	2518	14.47	369 524	2737	21.54
pcb3038	137 694	168 257	2946	22.69	187 563	2972	26.12

[a]BKS: best-known solution.
[b]BFS: best-found solution.

comparison, a GA, say GA-I, is developed with roulette wheel selection, cyclic crossover and random mutation. Table 3 presents the results of VLGA with GA-I. In terms of objective value, number of iterations and CPU time (results using 90 independent runs), VLGA performs better.

5.2. Statistical test (ANOVA)

In this investigation, assumptions of ANOVA (normal population distribution, distributions having homogeneous variance and independent data) are satisfied. To establish the supremacy of VLGA, we perform ANOVA. For this purpose, alongwith VLGA and GA-I, another algorithm GA-II with rank selection, cyclic crossover and random mutation is considered. Eleven standard test functions are evaluated by the algorithms VLGA, GA-I, and GA-II for a maximum of 2500 iterations. The number of wins (optimal results) of 100 independent runs of the above algorithms against the said test functions are recorded (cf. Table 4). Thus, for comparison of the above three algorithms, the difference between the two related sample means is tested.

From the standard table, the critical F values are $F_{0.05(2,30)} \approx 3.31$. This value is much less than the calculated F (=21.73) from Table 6. Significant differences exist between the groups. As the F-ratio is observed to be significant in the ANOVA test with two groups, it is essential to determine which group-means differ significantly from each other, and for that, a multiple-comparison test is performed. Scheffe's multiple-comparison F test is executed to determine whether the groups (VLGA and GA-I) and/or (VLGA and GA-II) are significant.

For VLGA and GA-I, we calculate F values following $F = \frac{(\overline{X}_1 - \overline{X}_3)^2}{MS_W(\frac{1}{7}+\frac{1}{7})}$ = 13.37. Similarly, for VLGA and GA-II, F = 41.73. Here, both cal-

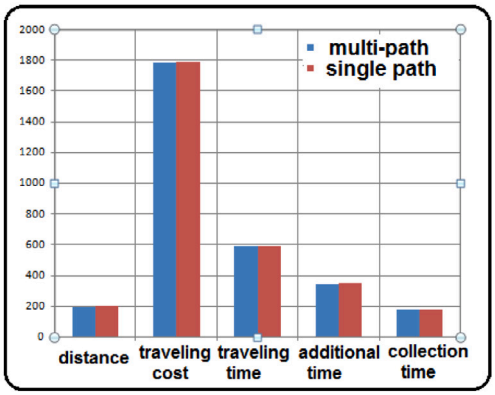

(a) Optimum results of Model A due to multi- and single path

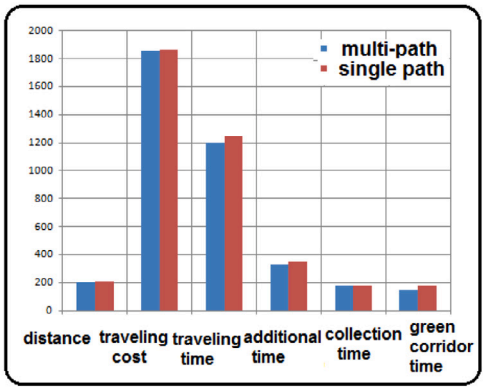

(b) Optimum results of Model B due to multi- and single path

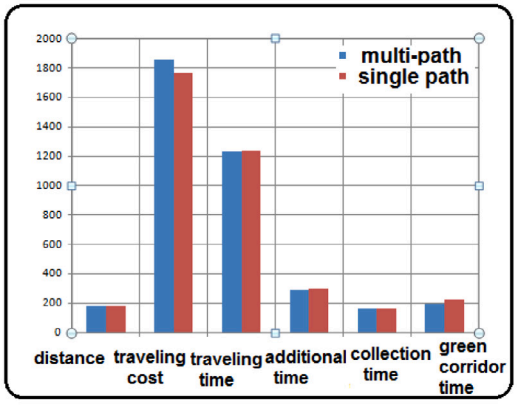

(c) Optimum results of Model C due to multi- and single path

Fig. 7. Different costs and time for Model A, B, and C.

Table 4
For different algorithms number of wins.

Problem	gr17	gr21	gr24	bays29	hk48	eil51	brazil58	st70	eil76	eil101	gr120
VLGA	76	84	71	80	75	83	88	81	72	78	65
GA-I	67	74	68	77	63	68	72	67	69	64	53
GA-II	61	69	58	62	61	54	63	62	58	60	42

Table 5
Data summary.

Groups	N	Mean	Std.Dev.	Std.Error
VLGA	11	77.54	6.62	1.99
GA-I	11	67.45	6.31	1.90
GA-II	11	59.09	6.77	2.04

culated values (13.37 and 41.73) of F are higher than the tabulated value of F (3.31); hence, significant differences exist for both groups. However, the mean of VLGA is higher than the other two means (Table 5). Therefore, it is concluded that VLGA is better than the other two algorithms, GA-I and GA-II.

Table 5 summarizes the data in above table. Here, the total number of problems is I = 11, and the total number of algorithms is J = 3. The mean of the sample means is $\overline{\overline{X}} = 68.02$.

6. A real-life experiment for MPC-19SCP

6.1. Different MPC-19SCPs with 10 nodes

We consider the case of COVID-19 specimen collection in the BANKURA district, West Bengal, India (cf. Fig. 1(a)). There is a main hospital-cum-testing center, Bankura Sammilani Medical College (marked by '0'), and 9 collection centers ((1) HLC Memorial, (2) Puncha, (3) Barjara, (4) Mission, (5) Gangajalghati,(6) Dubrajpur, (7) Ramsagar, (8) Sanaka Hospital, and (9) Health World). Thus, MPC-19SCPs are formulated following the 3DTSP procedure with 10 centers and 3 alternative routes between every two centers (cf. Section 3). The data for distances, travel costs per unit distance, travel times (for Model A), travel times (for Models B and C) and additional time matrices (rowwise 1st, 2nd, 3rd, 4th, and 5th) are presented in Table 14. Here, the travel times of Model A differ from those of Models B and C, and the remaining input data are the same for all the models. These data are used to illustrate Models A, B, and C. As mentioned earlier, there

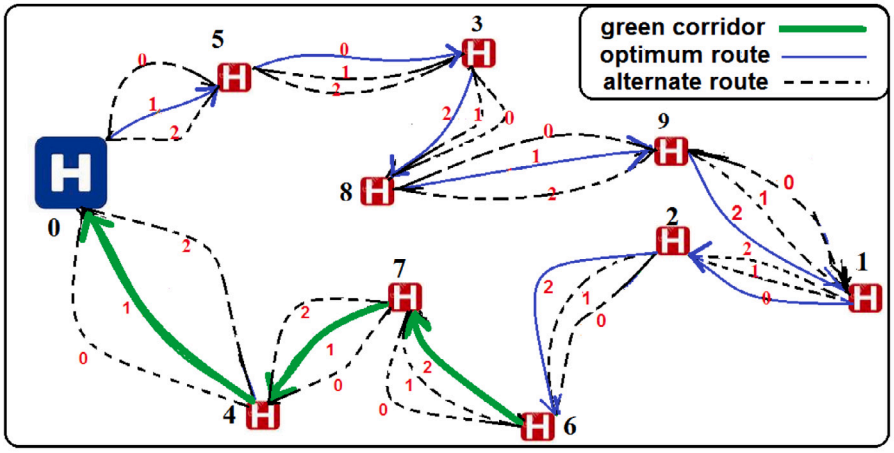

Fig. 8. Optimal path for Model B using green corridor.

Table 6
ANOVA summary table.

Source of variation	Sum of square	df	Mean of square	F
Between groups	SS_B = 1878.61	J-1 = 2	$MS_B = \frac{SS_B}{J-1}$ = 939.30	
Within groups	SS_W = 1296.36	J(I-1) = 30	$MS_W = \frac{SS_W}{J(I-1)}$ = 43.21	$\frac{MS_B}{MS_W}$ = 21.73
Total	SS_T = 3174.97	IJ-1 = 32		

Table 7
Experimental setup.

Parameters	Value/Range	Parameters	Value/Range
Number of chromosome	200	p_c	0.33
Max_Generation	2500	p_m	0.12
Number of nodes	10	T^f	24 h

Table 8
Results of all scenarios of Model A of MPC-19SCP.

Model A	Multipath	Single-path (1st path)
Path	0(2)-5(0)-3(0)-4(2) -8(2)-9(1)-1(0) -2(2)-6(1)-7(2)-0	0(0)-4(0)-9(0)-1(0) -2(0)-6(0)-7(0) -8(0)-3(0)-5(0)-0
Travel distance (km)	194	199
Travel cost (INR)	1783	1797
Travel time (min)	592	594
Additional time (min)	344	350
Specimens LT (min)	180	180
Total time (min)	1116	1124

LT: loading time.

Table 9
Results of all scenarios of Model B of MPC-19SCP.

Model B	Multipath	Single path (1st path)
Path	0(1)-5(0)-3(2)-8(1) -9(2)-1(0)-2(2) -6(2)-7(1)-4(1)-0	0(0)-4(0)-8(0)-3(0) -7(0)-6(0)-2(0) -1(0)-9(0)-5(0)-0
Travel distance (km)	202	206
Travel cost (INR)	1858	1868
Travel time (min)	1200	1246
Additional time (min)	332	350
Specimens LT (min)	180	180
Total time (min)	1712	1776
Routing time (min) after First specimens collection	1558	1598
Green corridor time require (min)	118	158
Green corridor time (min)	122	161
Green corridor segment (G')	6(2)-7 7(1)-4 4(1)-0 ...	2(0)-1 1(0)-9 9(0)-5 5(0)-0
Number of green corridor used	3	4

LT: loading time.

are three types of routes between every two centers including depot and centers with the corresponding distances, travel costs, travel times and additional time matrices. For the distance, travel cost, travel time and additional time (a,b,c), the values a, b and c are for the 1st, 2nd and 3rd routes, respectively. The specimen loading times are given in Table 15. With these data, we solve Model A (Eqs. (5)–(7)), B (Eqs. (9)–(12)), and C (Eqs. (14)–(19)) using the developed VLGA.

We perform these experiments with the parametric values given in Table 7. Here, we coded the algorithm in C and C++ using the Codeblock compiler on a 6th Generation Intel Core i3 CPU @ 3 GHz and 4 GB RAM.

6.1.1. Optimum results and discussion

The optimum results of Models A, B, and C of MPC-19SCP solved by VLGA are presented in Tables 8, 9, and 10, respectively. For each model, the optimum routing path, total distance, travel cost, travel time, additional time, specimen loading time, total system time, and routing time (after the collection of first specimen) are presented. The 'false-negative' of the specimens, T^f, is taken as 24 h.

6.1.2. Results of model A

For Model A, the optimal routing path is 0(2)-5(0)-3(0)-4(2)-8(2)-9(1)-1(0)-2(2)-6(1)-7(2)-0. This means that the collection vehicle starts from 0 (depot), moves to the 5th center using the 3rd path, and then moves to the 3rd center using the 1st path, after which it moves to the 4th center through the 1st path and so on. Here, alternate paths between two centers are represented by 0, 1 and 2. Distance, travel cost and total system time are 194 km, INR 1783 and 1116 min (travel time (592 min) + additional time (344 min) + specimen loading time (180 min), respectively) (cf. Fig. 7(a)). Instead of 3 routes, if there is a single route, say the 1st route (denoted by 0), then the optimum results of Model A are evaluated and presented in Table 8. It is observed that the multipath model performs better.

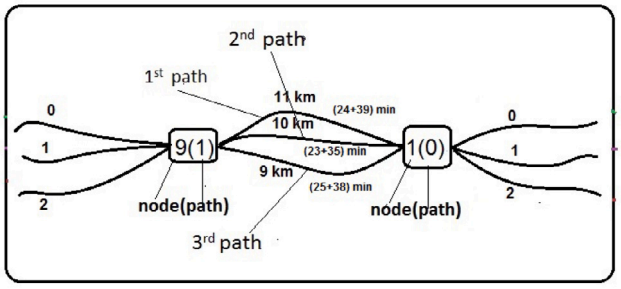

(a) Justification of multipath example 1

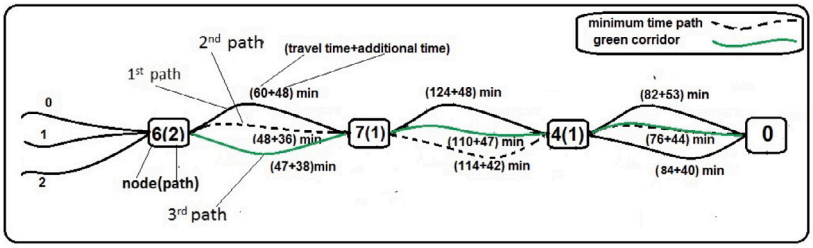

(b) Justification of multipath example 2

Fig. 9. Justification of multipath.

Table 10
Results of all scenarios of Model C of MPC-19SCP.

Model C	Multipath	Single path (1st path)
Path	0(0)-4(2)-5(0)-3(0)	0(0)-5(0)-1(0)-9(0)
	-2(1)-1(2)-8(2)	-7(0)-6(0)-8(0)
	-9(0)-7(2)-0	-3(0)-4(0)-0
Travel distance (km)	178	181
Travel cost (INR)	1746	1767
Travel time (min)	1228	1237
Additional time (min)	293	296
Specimens *LT* (min)	162	165
Total time (min)	1683	1698
Routing time (min) after		
First specimens collection	1631	1653
Green corridor time require (min)	191	213
Green corridor time (min)	197	221
Green corridor segment (G')	1(2)-8	7(0)-6
	8(2)-9	6(0)-8
	9(0)-7	8(0)-3
	7(2)-0	3(0)-4
		4(0)-0
Number of green corridor used	4	5
Asking center to send specimens	6	2
Minimum cost from asking centers	96 [6(0)-7]	121 [2(0)-6]

LT: loading time.

6.1.3. Results of model B

In Model B, the collection vehicle collects specimens from all the health centers using the green corridor and satisfying the 'false-negative' constraint. The optimal path of Model B is 0(1)-5(0)-3(2)-8(1)-9(2)-1(0)-2(2)-6(2)-7(1)-4(1)-0, corresponding to a time of 1712 min and a cost of INR 1858 (cf. Table 9 and Fig. 7(b)). The number of green corridor segments (G') among the centers is 3 (among centers 6(2)-7, 7(1)-4, and 4(1)-0). The green corridor and the overall optimal routing path are shown in Fig. 8. Similar to Model A, a scenario is observed for Model B with a single path (between centers). However, in this case (single path), the number of green corridor segments (G') among the centers increases to 4. In all the models, it is observed that the multipath models perform better than the single-path models.

6.1.4. Results of model C

In Model C, the collection vehicle collects specimens from all the health centers visiting the maximum possible number of centers through the green corridor system, asking some centers (not visited) to send their specimens to nearby centers lying on the green corridor and satisfying the 'false-negative' constraint. Here, the optimal path of Model C is 0(0)-4(2)-5(0)-3(0)-2(1)-1(2)-8(2)-9(0)-7(2)-0, corresponding to a time of 1683 min and a cost of INR 1746 (cf. Table 10 and Fig. 7(c)). Here, center 6 is a left-out (not visited) center, which is requested to send the specimens to nearby center 7, and the number of green corridor segments (G') among the centers is 4 among centers 1(2)-8, 8(2)-9, 9(0)-7, and 7(2)-0. Similar to Model B, a scenario is observed for Model C with a single path (between centers). However, in this case, the number of green corridor segments (G') among the centers is increased to 5. Here, 6 centers are asked to send specimens for multiple paths and 2 for a single path, and the corresponding costs incurred are INR 96 and INR 121, respectively. In all the models, it is observed that the multipath models perform better than the single-path models.

6.1.5. Justification of multipath

The use of multipath in a routing model is more realistic due to infrastructural development throughout the world, even in developing counties such as India. Here, for the first time, we have considered the availability of three different connecting paths between two arbitrary nodes. The optimum results of Models A, B, and C with multiple paths are better than those of the models with a single path (cf. Tables 8, 9, and 10). With multipath, the total system time and cost are less for Model A, and the green corridor times required for Models B and C are less (cf. Sections 6.1.2, 6.1.3, 6.1.4).

Let us consider the optimal path of Model A (with multipath), i.e., 0(2)-5(0)-3(0)-4(2)-8(2)-9(1)-1(0)-2(2)-6(1)-7(2)-0.

Here, (in Fig. 9), a travel path segment is 9(1)-1(0), i.e, the 2nd path is used among three alternate paths between nodes 9 and 1. Here, the distance between nodes is 10 km, and the time (travel+additional) is 58(23 + 35) min. As an alternative, if we consider only a single path between nodes 9 and 1, say the first path (0), the distance is increased by 1 km, and the time increases by 5 min, i.e., 63(24 + 39) min. For the

Table 11
Results of all scenarios of Model A of MPC-19SCP with 40 nodes.

Model A	Multipath	Single-path (1st path)
Path	0(2)-35(2)-10(0)-25(2)-30(2) -5(0)-33(2)-28(0)-4(2)-38(0) 24(2)-8(0)-14(2)-18(0)-34(0) -23(2)-15(2)-3(0)-32(2)-6(0) 37(0)-36(2)-17(2)-26(0)-2(2) -21(0)-29(0)-1(2)-39(2)-31(0) 19(2)-11(0)-13(2)-20(2)-12(0) -7(2)-16(0)-27(0)-22(0)-9(2)-0	0(0)-5(0)-10(0)-25(0)-30(0) -35(0)-20(0)-4(0)-28(0)-24(0) 8(0)-14(0)-18(0)-33(0)-15(0)- 23(0)-34(0)-38(0)-3(0)-21(0) 39(0)-22(0)-36(0)-37(0)-13(0)- 2(0)-26(0)-7(0)-16(0)-27(0) 6(0)-17(0)-12(0)-11(0)-29(0)- 32(0)-31(0)-9(0)-1(0)-19(0)
Travel distance (km)	196	202
Travel cost (INR)	1715	1746
Travel time (min)	585	591
Additional time (min)	362	374
Specimens *LT* (min)	270	270
Total time (min)	1217	1235

LT: loading time.

Table 12
Results of all scenarios of Model B of MPC-19SCP with 40 nodes.

Model B	Multipath	Single path (1st path)
Path	0(0)-1(2)-29(0)-36(2)-37(2)- 16(1)-10(2)-5(0)-24(1)-34(0) 6(1)-4(0)-13(2)-3(2)-21(1)- 19(1)-28(2)-18(2)-9(1)-8(1) 30(1)-35(2)-23(0)-32(0)-7(2)- 39(2)-27(1)-31(2)-38(0)-33(1) 25(2)-15(1)-22(2)-17(0)-2(2)- 20(0)-12(0)-26(0)-11(2)-14(0)-0	0(0)-25(0)-10(0)-14(0)-23(0)- 34(0)-20(0)-21(0)-1(0)-16(0) 29(0)-31(0)-19(0)-11(0)-39(0)- 8(0)-4(0)-13(0)-15(0)-27(0) 7(0)-28(0)-24(0)-6(0)-37(0)- 33(0)-35(0)-30(0)-5(0)-36(0) 9(0)-38(0)-3(0)-32(0)-26(0)- 12(0)-22(0)-17(0)-18(0)-2(0)-0
Travel distance (km)	209	221
Travel cost (INR)	1912	1934
Travel time (min)	1251	1317
Additional time (min)	346	378
Specimens *LT* (min)	270	270
Total time (min)	1867	1965
Routing time (min) after First specimens collection	1632	1712
GC time require (min)	192	272
GC time (min)	203	286
GC segment (G')	7(2)- 39(2)-27(1)-31(2)-38(0)-33(1) 25(2)-15(1)-22(2)-17(0)-2(2)- 20(0)-12(0)-26(0)-11(2)-14(0)-0	28(0)-24(0)-6(0)-37(0)- 33(0)-35(0)-30(0)-5(0)-36(0) 9(0)-38(0)-3(0)-32(0)-26(0)- 12(0)-22(0)-17(0)-18(0)-2(0)-0
Number of GC used	16	19

LT: loading time, GC: green corridor.

third path (2), the distance is reduced by 1 km, but the time increases by 5 min, i.e., 63(25 + 38) min. Therefore, the multipath/alternate path gives better routing for optimization.

Again, consider (in Fig. 9(b)) the optimal path of Model B, i.e., 0(1)-5(0)-3(2)-8(1)-9(2)-1(0)-2(2)-6(2)-7(1)-4(1)-0. Here, the minimum time path is shown by the dotted line, and the green corridor is shown by the green line. As the total time between two arbitrary centers is based on travel time + additional time, when a green corridor is imposed, the additional times are eliminated. The times between the 6th and 7th centers using the first, second and third paths are 108(60 + 48), 84(48 + 36) and 85(47 + 38), respectively. Therefore, when routing with minimum time is performed, the second path is selected, but when the green corridor is imposed, the third path is selected, as the third path contains less travel time (47) as we eliminate additional time from the path. Similarly, from center 7 to 4, although the third path (156) takes less time than the second path (157), a green corridor is imposed on the second path. However, for center 4 to the main hospital (0), the minimum time path and green corridor path are the same. Therefore, multiple paths play an important role in this investigation.

6.1.6. Justification of the green corridor

As the present investigation is related to disease control scenarios, it is expected that the collection vehicle(s) should collect specimens from all health centers. During travel, congestion, traffic signals, festival processions, etc. (termed 'additional time'), routing time is wasted. The green corridor arrangement (by police or some other government authority) saves these 'additional times', allowing the vehicle to make a nonstop run. However, in this process, some public hindrances, such as stopping public transit, are automatically created. Therefore, attempts should be made to (i) increase specimen collections using green corridors and (ii) minimize public inconvenience, i.e., green corridor time. As a solution, a green corridor can be applied. For smooth management, green corridors, are normally applied toward the end of the journey. Thus, we apply the necessary green corridor toward the end of the routing path, i.e., the contiguous collecting centers up to the main hospital, necessary to cover the maximum number of centers for specimen collection within 'false negativity'. In Model B, to take specimens from all centers, a green corridor is applied for 118 min in the last three intervals (6(2)-7, 7(1)-4, 4(1)-0).

6.2. Real-life MPC-19SCPs with 40 nodes/centers

6.2.1. Input data

All the relevant input data are available at https://github.com/somnathmajivucs/COVID-19_40nodes_input_data.

6.2.2. Optimum results

As in Section 6.1, the optimum results of Models A, B, and C are evaluated and presented in Tables 11–13 and Figs. 10 and 11.

Discussions of the models are the same as those presented in Section 6.1.

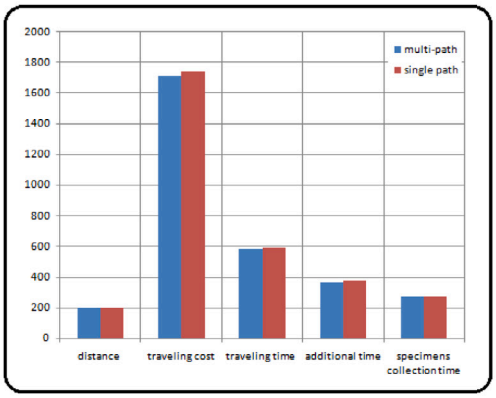

(a) Optimum results of Model A due to multi- and single path

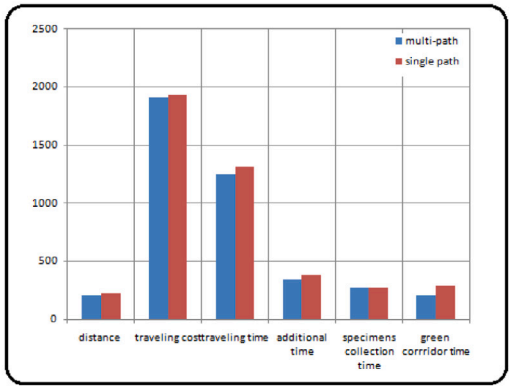

(b) Optimum results of Model B due to multi- and single path

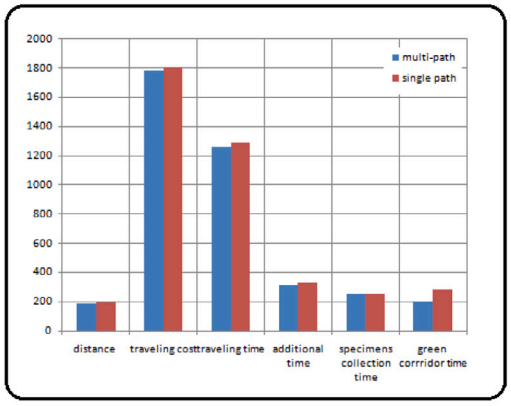

(c) Optimum results of Model C due to multi- and single path

Fig. 10. Different cost and time for Model A, B and C with 40 nodes.

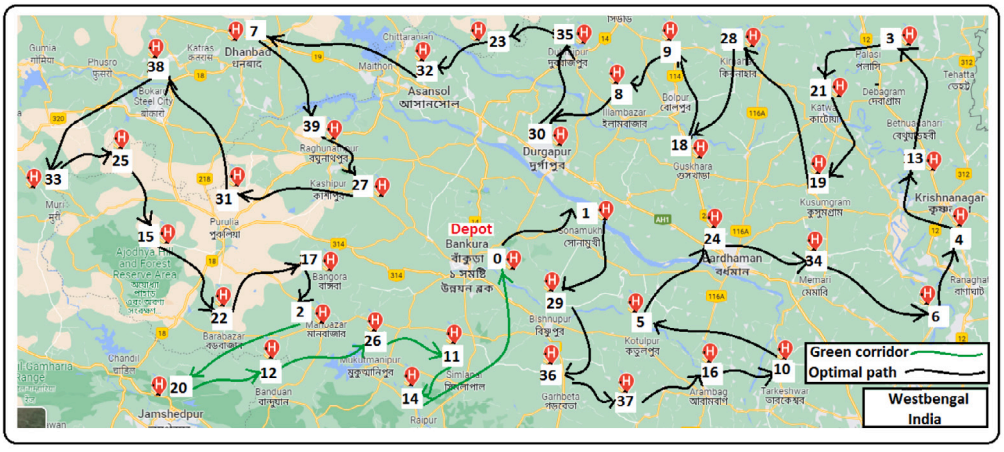

Fig. 11. Optimal path for Model B using green corridor with 40 nodes.

Table 13
Results of all scenarios of Model C of MPC-19SCP with 40 nodes.

Model C	Multipath	Single path (1st path)
Path	0(2)-35(2)-10(0)-25(2)- 5(0)-33(2)-28(0)-4(2)-38(0) 24(2)-8(0)-18(0)-34(0)- 23(2)-3(0)-32(2)-6(0) 37(0)-36(2)-17(2)-26(0)-2(2)- 21(0)-29(0)-1(2)-39(2)-31(0) 19(2)-11(0)-13(2)-20(2)-12(0)- 7(2)-16(0)-27(0)-22(0)-9(2)-0	0(0)-4(0)-28(0)-13(0)- 36(0)-2(0)-22(0)-39(0) 1(0)-12(0)-19(0)-31(0)- 18(0)-24(0)-38(0)-34(0)-30(0) 14(0)-8(0)-29(0)-7(0)- 16(0)-17(0)-26(0)-27(0)-23(0) 25(0)-10(0)-5(0)-33(0)-15(0)- 3(0)-32(0)-9(0)-20(0)-37(0)-0
Travel distance (km)	186	192
Travel cost (INR)	1781	1803
Travel time (min)	1262	1291
Additional time (min)	316	329
Specimens *LT* (min)	254	256
Total time (min)	1832	1876
Routing time (min) after First specimens collection	1784	1805
GC time require (min)	344	365
GC time (min)	349	371
GC segment (G')	 4(2)-38(0) 24(2)-8(0)-18(0)-34(0)- 23(2)-3(0)-32(2)-6(0) 37(0)-36(2)-17(2)-26(0)-2(2)- 21(0)-29(0)-1(2)-39(2)-31(0) 19(2)-11(0)-13(2)-20(2)-12(0)- 7(2)-16(0)-27(0)-22(0)-9(2)-0	13(0)- 36(0)-2(0)-22(0)-39(0) 1(0)-12(0)-19(0)-31(0)- 18(0)-24(0)-38(0)-34(0)-30(0) 14(0)-8(0)-29(0)-7(0)- 16(0)-17(0)-26(0)-27(0)-23(0) 25(0)-10(0)-5(0)-33(0)-15(0)- 3(0)-32(0)-9(0)-20(0)-37(0)-0
Number of GC used	31	33
Asking center to Send specimens	14, 15, 30	21, 35, 6, 11
Min cost from	[14(2)-8]	[21(0)-19]
Asking centers	[15(2)-17] [30(1)-13]	[35(0)-9] [6(0)-37] [11(0)-20]

LT: loading time, GC: green corridor.

7. Conclusion

7.1. General comments

In the present investigation, considering the resource constraints (number of medical vans) of rural hospitals of developing countries, such as India, it is assumed that only one medical van is available for specimen collection. Here, some models (MPC-19SCPs) are proposed to collect COVID-19 specimens from all remote health centers to bring to medical center for testing in minimum time, satisfying the first collected specimen's 'false-negative' constraint. A vehicle starts from the main hospital and returns to it after collection following an optimum routing plan. There are several connecting paths among the centers and also between the main hospital and the centers.

In Model A, collection from all centers is possible, satisfying the 'false-negative' constraint of the first collected specimen. In Models B and C, collection from all centers is not possible within the 'false-negative' constraint. As this is an investigation to control disease, specimens from all centers must be collected, and keeping this in mind, we propose two alternatives: (iia) To minimize public hindrance, we minimize the green corridor time to cover all health centers within the 'false-negative' time, if possible (Model B). (iib) After the green corridor is introduced, if it is not possible to cover all health centers within the 'false-negative' time, then we maximize the number of visited centers, and the remaining (minimum) centers are asked to send their specimens to the nearest visited centers lying on the green corridor (Model C). For the solution, variable-length chromosome GA is developed and used.

Thus, the contributions of the present investigation are twofold: (i) It develops a real-life specimen collection problem under different disease control scenarios satisfying the 'false-negative' constraint. The use of the 'green corridor' concept for this purpose is new in the literature. (ii) It develops variable-length chromosome GA with probabilistic selection, sequence-based comparison crossover and generation-dependent mutation in connection with the collection of medical specimens with a finite life time. The concept of sequence-based comparison crossover is newly introduced in GA. The validity and supremacy of VLGA are established through the testing of benchmark functions and ANOVA.

The developed MPC-19SCP models can be modified and solved taking a specific country's present testing and collection procedures into account. If the resources (availability of multiple medical vans) permit, the present problem can be formulated as a multiple vehicle routing problem (MVRP) and solved. The developed algorithm, VLGA, is in general form and can be applied in other TSP-type problems, such as the VRP, TPP, Facility Location Problem, Disaster Management Problem, etc.

7.2. Limitations

The limitations of the present investigation are that (i) only one vehicle is considered for collection (routing) due to resource constraints, (ii) the capacity of the vehicle is considered sufficient to accommodate all collected specimens (The vehicle may be taken to have finite capacity), (iii) the green corridor is imposed sequentially toward the end of the path, which can be applied anywhere on the routing path depending on the prevailing circumstances, and (iv) due to the use of sequence-based comparison crossover in VLGA, large problems require more computation time. For real-life illustration, two MPC-19SCP examples, one with 10 nodes and another with 40 nodes, are considered and solved. In the model formulation, the possibility of an accident involving the medical vehicle and risks due to the spread of infection, etc., are not considered.

7.3. Future research scopes

In the future, (i) MPC-19SCP models with time windows can also be formulated and solved, (ii) green corridors may be imposed as per

Table 14
Input data: Distance (in km), travel cost per unit distance (INR), travel time (min) (for Model A), travel time (min) (for Model B, and C) and additional time (min).

i/j	0	1	2	3	4	5	6	7	8	9
		(29,27,33)	(32,30,27)	(37,34,32)	(18,26,21)	(18,16,14)	(37,40,35)	(39,35,32)	(42,47,44)	(32,29,26)
		(10,11,8)	(9,8,11)	(8,9,10)	(9,7,11)	(8,9,10)	(11,9,8)	(9,8,11)	(7,9,11)	(9,10,7)
0	∞	(288,276,292)	(290,286,278)	(308,298,294)	(252,272,262)	(250,246,238)	(314,318,302)	(318,310,304)	(326,338,332)	(302,296,290)
		(144,138,146)	(145,143,139)	(154,149,147)	(126,136,131)	(125,123,119)	(157,159,151)	(159,155,152)	(163,169,166)	(151,148,145)
		(40,38,37)	(30,35,33)	(36,39,30)	(32,34,36)	(32,31,30)	(39,32,39)	(38,44,39)	(36,33,35)	(39,30,35)
	(29,27,33)		(22,26,28)	(30,26,31)	(37,36,38)	(48,46,43)	(32,36,33)	(44,46,47)	(30,26,25)	(13,15,17)
	(10,11,8)		(8,9,8)	(9,10,11)	(8,10,9)	(7,9,10)	(11,10,9)	(8,9,8)	(7,10,8)	(11,10,9)
1	(288,276,292)	∞	(266,278,282)	(290,276,294)	(310,306,334)	(318,338,330)	(292,306,300)	(330,334,338)	(292,278,274)	(248,246,250)
	(144,138,146)		(133,139,141)	(145,138,147)	(155,153,167)	(159,169,165)	(146,153,150)	(165,167,169)	(146,139,137)	(124,123,125)
	(40,38,37)		(30,40,32)	(30,35,37)	(37,39,31)	(30,37,39)	(36,38,42)	(32,34,45)	(36,38,36)	(39,35,38)
	(32,30,27)	(22,26,28)		(32,36,39)	(27,26,23)	(37,39,41)	(11,16,15)	(34,38,35)	(42,44,47)	(32,37,34)
	(9,8,11)	(8,9,8)		(8,10,10)	(9,7,11)	(10,9,8)	(11,9,9)	(10,9,10)	(8,8,8)	(9,8,10)
2	(290,286,278)	(266,278,282)	∞	(96,108,116)	(80,78,66)	(108,112,126)	(23,48,13)	(98,114,104)	(130,134,140)	(294,310,300)
	(145,143,139)	(133,139,141)		(148,154,158)	(140,139,133)	(154,156,163)	(116,124,123)	(149,157,152)	(165,167,170)	(147,155,150)
	(30,35,33)	(30,40,32)		(39,40,37)	(39,42,37)	(45,38,33)	(35,40,41)	(35,36,47)	(39,42,38)	(30,32,27)
	(37,34,32)	(30,26,31)	(32,36,39)		(22,26,28)	(27,26,28)	(32,36,35)	(37,36,40)	(24,26,22)	(39,36,34)
	(8,9,10)	(9,10,11)	(8,10,10)		(9,8,10)	(7,9,9)	(8,10,9)	(9,9,10)	(8,9,10)	(9,8,9)
3	(308,298,294)	(90,78,94)	(96,108,116)	∞	(68,76,82)	(80,76,82)	(94,106,104)	(108,106,120)	(70,76,66)	(314,308,300)
	(154,149,147)	(145,139,147)	(148,154,158)		(134,138,141)	(140,138,141)	(147,153,152)	(154,153,160)	(135,138,133)	(157,154,150)
	(36,39,30)	(42,45,36)	(39,40,37)		(33,35,39)	(35,38,38)	(33,39,36)	(30,35,39)	(41,39,20)	(35,37,40)
	(18,26,21)	(37,36,38)	(27,26,23)	(22,26,28)		(22,26,24)	(23,26,28)	(32,36,38)	(16,16,18)	(30,36,31)
	(9,7,11)	(8,9,10)	(9,7,11)	(9,8,10)		(10,9,10)	(9,8,7)	(9,10,8)	(7,9,9)	(8,10,9)
4	(252,272,262)	(106,108,134)	(78,76,70)	(68,76,82)	∞	(68,76,70)	(68,78,82)	(96,108,112)	(48,48,52)	(290,308,294)
	(126,136,131)	(153,154,157)	(139,138,135)	(134,138,141)		(134,138,135)	(134,139,141)	(148,154,156)	(124,124,126)	(145,154,147)
	(32,34,36)	(35,42,40)	(30,32,36)	(33,35,39)		(34,39,37)	(32,36,38)	(42,46,40)	(42,43,37)	(42,33,37)
	(18,16,14)	(48,46,43)	(37,39,41)	(27,26,28)	(22,26,24)		(34,36,38)	(42,46,47)	(34,36,38)	(32,36,20)
	(8,9,10)	(7,9,10)	(10,9,8)	(7,9,9)	(10,9,10)		(7,8,8)	(9,9,11)	(10,9,8)	(8,9,9)
5	(250,246,238)	(136,132,126)	(108,118,126)	(78,80,84)	(68,76,70)	∞	(98,108,116)	(124,132,136)	(100,108,118)	(296,306,290)
	(125,123,119)	(168,166,163)	(154,159,163)	(139,140,142)	(134,138,135)		(149,154,158)	(162,166,168)	(150,154,159)	(148,153,145)
	(32,31,30)	(30,34,38)	(42,36,39)	(38,45,38)	(34,39,37)		(32,35,37)	(33,40,37)	(40,42,35)	(36,38,39)
	(37,40,35)	(32,36,33)	(11,16,15)	(32,36,35)	(23,26,28)	(34,36,38)		(12,16,13)	(34,36,32)	(22,26,20)
	(11,9,8)	(11,10,9)	(11,9,9)	(8,10,9)	(9,8,7)	(7,8,8)		(8,9,8)	(10,10,9)	(11,9,8)
6	(314,318,302)	(92,108,98)	(38,48,44)	(94,108,104)	(70,78,84)	(98,108,116)	∞	(60,48,47)	(100,104,94)	(268,278,260)
	(157,159,151)	(146,154,149)	(119,124,122)	(147,154,152)	(135,139,142)	(149,154,158)		(124,120,121)	(150,152,147)	(134,139,130)
	(39,32,39)	(38,43,36)	(35,40,37)	(42,44,39)	(44,41,37)	(32,35,37)		(48,36,38)	(45,44,33)	(44,42,35)
	(39,35,32)	(44,46,47)	(34,38,35)	(37,36,40)	(32,36,38)	(42,46,47)	(12,16,13)		(24,26,25)	(39,36,42)
	(9,8,11)	(8,9,8)	(10,9,10)	(9,9,10)	(9,10,8)	(9,9,11)	(8,9,8)		(9,8,10)	(10,9,11)
7	(318,310,304)	(128,132,134)	(100,132,104)	(108,110,120)	(124,110,114)	(124,132,134)	(60,48,47)	∞	(70,78,74)	(316,308,326)
	(159,155,152)	(164,166,167)	(150,156,152)	(154,155,160)	(157,155,147)	(162,166,167)	(124,120,121)		(135,139,137)	(158,154,164)
	(38,44,39)	(33,31,47)	(30,35,39)	(39,38,32)	(48,47,42)	(32,44,40)	(48,36,38)		(38,43,36)	(32,37,45)
	(42,47,44)	(30,26,25)	(42,44,47)	(24,26,22)	(16,16,18)	(34,36,38)	(34,36,32)	(24,26,25)		(30,26,25)
	(7,9,11)	(7,10,8)	(8,8,8)	(8,9,10)	(7,9,9)	(10,9,8)	(10,10,9)	(9,8,10)		(9,11,10)
8	(326,338,332)	(90,78,74)	(124,128,134)	(72,78,68)	(48,48,52)	(100,108,108)	(100,108,94)	(70,78,74)	∞	(290,278,274)
	(163,169,166)	(145,139,137)	(162,164,167)	(136,139,134)	(124,124,126)	(150,154,154)	(150,154,147)	(135,139,137)		(145,139,137)
	(36,33,35)	(38,32,47)	(35,30,36)	(35,44,34)	(42,38,37)	(38,40,46)	(36,32,40)	(38,43,36)		(40,39,38)
	(32,29,26)	(13,15,17)	(32,37,34)	(39,36,34)	(30,36,31)	(32,36,20)	(22,26,20)	(39,36,42)	(30,26,25)	
	(9,10,7)	(11,10,9)	(9,8,10)	(9,8,9)	(8,10,9)	(8,9,7)	(11,9,8)	(10,9,11)	(9,11,10)	
9	(302,296,290)	(248,246,250)	(294,310,300)	(314,308,300)	(290,308,294)	(296,306,290)	(268,278,260)	(316,308,328)	(290,278,274)	∞
	(151,145,145)	(124,123,125)	(147,155,150)	(157,154,150)	(145,154,147)	(148,153,145)	(134,139,130)	(158,154,164)	(145,139,137)	
	(39,30,35)	(39,35,38)	(30,32,27)	(35,37,40)	(42,33,37)	(36,38,39)	(44,42,35)	(32,37,45)	(40,39,38)	

Table 15
Specimens loading matrix.

	Specimens loading time (min)									
Center	0	1	2	3	4	5	6	7	8	9
Loading time	0	30	15	9	12	36	18	6	30	24

requirements and prevailing situation, and (iii) different discrete operations for VLGA may be investigated. Risks of spreading infection, etc., due to the collision/accident of vehicles carrying COVID-19 specimens among the people of that locality may be considered.

CRediT authorship contribution statement

Somnath Maji: Conceptualization, Methodology, Software, Writing – original draft. **Kunal Pradhan:** Conceptualization, Validation, Methodology, Software. **Samir Maity:** Validation, Software, Writing, Writing – review & editing, Writing – original draft. **Izabela Ewa Nielsen:** Supervision, Validation, Review - original draft. **Debasis Giri:** Supervision, Validation. **Manoranjan Maiti:** Conceptualization, Supervision, Validation, Writing – review & editing.

Declaration of competing interest

The authors declare that they have no known competing financial interests or personal relationships that could have appeared to influence the work reported in this paper.

Funding

No funding was received for conducting this study.

Ethics approval

This article does not contain any studies with human participants or animals performed by any of the authors.

Code availability

System: Windows 2010, CPU: CORE i5, RAM: 4 GB, Software: C++ (Code Block), MATLAB,.

Informed consent

Informed consent was obtained from all individual participants included in the study.

Consent for publication

The manuscript has not been sent to any other journal for publication.

References

Abu-Monshar, A., Al-Bazi, A., & Palade, V. (2022). An agent-based optimisation approach for vehicle routing problem with unique vehicle location and depot. *Expert Systems with Applications*, *192*, Article 116370.

Adigal, S. S., Rayaroth, N. V., John, R. V., Pai, K. M., Bhandari, S., Mohapatra, A. K., Lukose, J., Patil, A., Bankapur, A., & Chidangil, S. (2021). A review on human body fluids for the diagnosis of viral infections: scope for rapid detection of COVID-19. *Expert Review of Molecular Diagnostics*, *21*(1), 31–42.

Anwit, R., & Jana, P. K. (2018). A variable length genetic algorithm approach to optimize data collection using mobile sink in wireless sensor networks. In *2018 5th international conference on signal processing and integrated networks* (pp. 73–77). IEEE.

Aringhieri, R., Bruni, M. E., Khodaparasti, S., & van Essen, J. T. (2017). Emergency medical services and beyond: Addressing new challenges through a wide literature review. *Computers & Operations Research*, *78*, 349–368.

Asturias, J., García-Santana, M., & Ramos, R. (2019). Competition and the welfare gains from transportation infrastructure: Evidence from the golden quadrilateral of India. *Journal of the European Economic Association*, *17*(6), 1881–1940.

Bellotti, H. B., & Francoso, M. T. (2021). System for transporting human organs. *Case Studies on Transport Policy*.

Bruni, M. E., Conforti, D., Sicilia, N., & Trotta, S. (2006). A new organ transplantation location–allocation policy: a case study of Italy. *Health Care Management Science*, *9*(2), 125–142.

Cruz-Piris, L., Marsa-Maestre, I., & Lopez-Carmona, M. A. (2019). A variable-length chromosome genetic algorithm to solve a road traffic coordination multipath problem. *IEEE Access*, *7*, 111968–111981.

Dhatrak, A., & Gandhe, S. (2018). Automatic traffic signals in smart cities for speedy clearance of emergency vehicles. In *2018 fourth international conference on computing communication control and automation* (pp. 1–6). IEEE.

Di Placido, A., Archetti, C., & Cerrone, C. (2022). A genetic algorithm for the close-enough traveling salesman problem with application to solar panels diagnostic reconnaissance. *Computers & Operations Research*, *145*, Article 105831.

Gamal, A., Abdel-Basset, M., & Chakrabortty, R. K. (2022). Intelligent model for contemporary supply chain barriers in manufacturing sectors under the impact of the COVID-19 pandemic. *Expert Systems with Applications*, Article 117711.

Halder, B., Bandyopadhyay, J., & Banik, P. (2022). Statistical data analysis of risk factor associated with mortality rate by COVID-19 pandemic in India. *Modeling Earth Systems and Environment*, *8*(1), 511–521.

Kannan, D., Gurusriram, R., Banerjee, R., Bhattacharjee, S., & Varadwaj, P. K. (2021). Will there be a third COVID-19 wave? A SVEIRD model-based study of India's situation. *Indian Journal of Physics*, *95*(11), 2513–2521.

Karpova, Y., Villa, F., Vallada, E., & Vecina, M. Á. (2023). Heuristic algorithms based on the isochron analysis for dynamic relocation of medical emergency vehicles. *Expert Systems with Applications*, *212*, Article 118773.

Kim, S., & Moon, I. (2018). Traveling salesman problem with a drone station. *IEEE Transactions on Systems, Man, and Cybernetics: Systems*, *49*(1), 42–52.

Kumar, A., Misra, S. C., & Chan, F. T. (2022). Leveraging AI for advanced analytics to forecast altered tourism industry parameters: A COVID-19 motivated study. *Expert Systems with Applications*, *210*, Article 118628.

Kuo, R., Edbert, E., Zulvia, F. E., & Lu, S.-H. (2023). Applying NSGA-II to vehicle routing problem with drones considering makespan and carbon emission. *Expert Systems with Applications*, Article 119777.

Maity, S., Roy, A., & Maiti, M. (2015). A modified genetic algorithm for solving uncertain constrained solid travelling salesman problems. *Computers & Industrial Engineering*, *83*, 273–296.

Nguyen, A. T., Brzezinski, M., Chen, J., Nguyen, N. V., Dinh, L. V., & Kukreja, J. (2020). Lung transplant programs in developing countries: challenges, solutions, and outcomes. *Current Opinion in Organ Transplantation*, *25*(3), 299–304.

Pawar, S. N., & Bichkar, R. S. (2015). Genetic algorithm with variable length chromosomes for network intrusion detection. *International Journal of Automation and Computing*, *12*(3), 337–342.

Perboli, G., & Arabnezhad, E. (2021). A machine learning-based DSS for mid and long-term company crisis prediction. *Expert Systems with Applications*, *174*, Article 114758.

Qiongbing, Z., & Lixin, D. (2016). A new crossover mechanism for genetic algorithms with variable-length chromosomes for path optimization problems. *Expert Systems with Applications*, *60*, 183–189.

Rahmanifar, G., Mohammadi, M., Sherafat, A., Hajiaghaei-Keshteli, M., Fusco, G., & Colombaroni, C. (2023). Heuristic approaches to address vehicle routing problem in the iot-based waste management system. *Expert Systems with Applications*, Article 119708.

Reinelt, G. (1991). TSPLIB—A traveling salesman problem library. *ORSA Journal on Computing*, *3*(4), 376–384.

Saji, Y., & Barkatou, M. (2021). A discrete bat algorithm based on Lévy flights for euclidean traveling salesman problem. *Expert Systems with Applications*, *172*, Article 114639.

Wagale, M., Singh, A. P., & Sarkar, A. K. (2020). Impact of rural road construction on the local livelihood diversification: Evidence from pradhan mantri gram sadak yojana in jhunjhunu district, India. *GeoJournal*, *85*, 961–978.

Walia, S. S., Somarathna, K., Hendricks, R., Jackson, A., & Nagarur, N. (2018). Optimizing the emergency delivery of medical supplies with unmanned aircraft vehicles. In *Proceedings of the 2018 IISE annual conference, Vol. 1* (pp. 952–957).

Wang, X., Choi, T.-M., Li, Z., & Shao, S. (2019). An effective local search algorithm for the multidepot cumulative capacitated vehicle routing problem. *IEEE Transactions on Systems, Man, and Cybernetics: Systems*, *50*(12), 4948–4958.

Wang, X., Choi, T.-M., Liu, H., & Yue, X. (2016). A novel hybrid ant colony optimization algorithm for emergency transportation problems during post-disaster scenarios. *IEEE Transactions on Systems, Man, and Cybernetics: Systems*, *48*(4), 545–556.

Wang, Y., & Wang, N. (2023). Moving-target travelling salesman problem for a helicopter patrolling suspicious boats in antipiracy escort operations. *Expert Systems with Applications*, *213*, Article 118986.

WHO (2020). Coronavirus disease (COVID-19) outbreak situation. Available online: https://www.who.int/emergencies/diseases/novel-coronavirus-2019/.

Zahiri, B., Tavakkoli-Moghaddam, R., & Pishvaee, M. S. (2014). A robust possibilistic programming approach to multi-period location–allocation of organ transplant centers under uncertainty. *Computers & Industrial Engineering*, *74*, 139–148.

Zhang, J., Li, Y., & Yu, G. (2022). Emergency relief network design under ambiguous demands: A distributionally robust optimization approach. *Expert Systems with Applications*, *208*, Article 118139.

Zhang, C., & Tian, Y.-X. (2022). Forecast daily tourist volumes during the epidemic period using COVID-19 data, search engine data and weather data. *Expert Systems with Applications*, *210*, Article 118505.

Zhang, P., Wang, J., Tian, Z., Sun, S., Li, J., & Yang, J. (2022). A genetic algorithm with jumping gene and heuristic operators for traveling salesman problem. *Applied Soft Computing*, *127*, Article 109339.

Zhang, T., Zhou, Y., Zhou, G., Deng, W., & Luo, Q. (2023). Discrete mayfly algorithm for spherical asymmetric traveling salesman problem. *Expert Systems with Applications*, Article 119765.

Ziya-Gorabi, F., Ghodratnama, A., Tavakkoli-Moghaddam, R., & Asadi-Lari, M. S. (2022). A new fuzzy tri-objective model for a home health care problem with green ambulance routing and congestion under uncertainty. *Expert Systems with Applications*, *201*, Article 117093.